Cancer Immunology, Immunotherapy (2023) 72:1779–1788
https://doi.org/10.1007/s00262-023-03369-8

RESEARCH

Prognostic role of the innate immune signature CD163 and "eat me" signal calreticulin in clear cell renal cell carcinoma

Tadatsugu Anno[1] · Nobuyuki Tanaka[1] · Kimiharu Takamatsu[1] · Kyohei Hakozaki[1] · Ryohei Kufukihara[1] · Yuto Baba[1] · Toshikazu Takeda[1] · Kazuhiro Matsumoto[1] · Shinya Morita[1] · Takeo Kosaka[1] · Shuji Mikami[2] · Hiroshi Nishihara[3] · Ryuichi Mizuno[1] · Mototsugu Oya[1]

Received: 26 September 2022 / Accepted: 5 January 2023 / Published online: 17 January 2023

Abstract

The effects of the innate immune status on patients with clear cell renal cell carcinoma (ccRCC) currently remain unknown. We herein provided more extensive information about the inner landscape of immunobiology of ccRCC. In total, 260 ccRCC samples from three different cohorts consisting of 213 primary tumors and 47 metastases were obtained. We focused on five representative innate immune signatures, CD68, CD163, the "eat me" signal calreticulin, the "don't eat me" signal CD47, and signal regulatory protein α, and examined the role of each signature by quantitative immunohistochemistry. We then conducted an integrated genome mutation analysis by next-generation sequencing. Among the five markers, high CD163 and low calreticulin expression levels were prognostic in ccRCC. The application of a new risk model based on CD163 and calreticulin levels, named the innate immune risk group (high risk: high-CD163/low calreticulin, intermediate risk: high-CD163/high calreticulin or low CD163/low calreticulin, low risk: low-CD163/high calreticulin), enabled the sequential stratification of patient prognosis and malignancy. Although organ-specific differences were observed, metastases appeared to have a higher innate immune risk, particularly in the lungs, with 50% of ccRCC metastases being classified into the high-risk group according to our risk score. An analysis of genomic alterations based on the innate immune risk group revealed that alterations in the TP53/Cell cycle pathway were highly prevalent in high-risk ccRCC patients according to two innate immune signatures CD163 and calreticulin. The present results provide insights into the immune-genomic biology of ccRCC tumors for innate immunity and will contribute to future therapies focused on the innate immune system in solid cancers.

Keywords Renal cell carcinoma · Kidney cancer · Innate immunity · CD163 · Tumor-associated macrophage · Calreticulin · Eat me signal · Survival

Introduction

Advances have been achieved in the systemic treatment of metastatic renal cell carcinoma (RCC) in the last decade [1]. Interferon-α and interleukin-2 are the most common treatments and have been used for more than 10 years. Since response rates to these modalities were insufficient [2, 3], molecular targeted therapy subsequently replaced interferon α and interleukin-2 as a second-generation therapy. Molecular targeted therapy in RCC targets vascular endothelial growth factor or mammalian target of rapamycin and achieves a higher response rate and longer progression-free survival than primitive immunotherapy [4–8]. Furthermore, metastatic RCC treatments have evolved, and a new paradigm shift in therapeutic strategies is clear, i.e., the emerging role of immune checkpoint inhibitors. Based on the success of the anti-PD-1 antibody nivolumab, drug development and clinical trials have been proceeded in the acquired immunity field with PD-1/PD-L1/CTLA-4 [9, 10].

Immune responses to cancer cells involve seven steps referred to as the cancer-immunity cycle [11, 12]. To enhance antitumor responses, various combinations of immune therapy have been applied, and the innate immune

✉ Nobuyuki Tanaka
urotanaka@keio.jp

[1] Department of Urology, Keio University School of Medicine, Tokyo 160-8582, Japan

[2] Department of Diagnostic Pathology, Keio University Hospital, Tokyo 160-8582, Japan

[3] Genomics Unit, Keio Cancer Center, Keio University School of Medicine, Tokyo, Japan

system is now attracting attention. Innate immunity functions as the first line of defense against cancer cells, which act as antigen-presenting cells, thereby resulting in acquired immunity. Clinical and preclinical trials targeting the innate immune system are currently ongoing [13–16], and properly activated macrophages play a central role in this mechanism. On the other hand, tumor-associated macrophages (TAMs) in the microenvironment promote genetic instability, the growth of cancer stem cells, support metastasis, suppress acquired immunity, and promote tumor growth and progression [17, 18]. Furthermore, in tumor innate immunity, the phagocytosis of macrophages depends on pro-phagocytic ("eat me") and anti-phagocytic ("don't eat me") signals. Calreticulin is an "eat me" signal and promotes the efferocytosis of apoptotic cells and removal of cancer cells [19]. CD47 is a "don't eat me" signal, and CD47 on tumor cells interacts with signal regulatory protein α (SIRPα) on macrophages, resulting in tumor evasion from phagocytosis by macrophages. Targeting of the CD47/SIRPα axis has been reported to induce robust anticancer activity against non-Hodgkin's lymphoma [14].

In rapidly evolving immuno-oncology, the elucidation of tumor innate immunity may be achieved in RCC, which is typical of immunotherapy for solid tumors. The effects of the innate immune status on patients with RCC currently remain unknown. Therefore, we herein examined clear cell RCC (ccRCC) tissue to clarify the relationship between innate immune signatures and ccRCC outcomes. We initially focused on five representative innate immune signatures, CD68 (labels all macrophages), CD163 (labels TAMs), the "eat me" signal calreticulin, the "don't eat me" signal CD47, and SIRPα, and then investigated the role of each signature in the tumor beds of ccRCC. We also assessed changes in altered genetic states that underlie the malignant innate immune signatures in ccRCC.

Materials and methods

Human samples

After approval by the Institutional Review Board, three different cohorts of ccRCC tumor samples obtained between 1999 and 2017 at Keio University Hospital (Tokyo, Japan) were retrospectively collected based on the pathological T stage and systemic therapy used. Details on the three groups are as follows: COHORT 1, 105 formalin-fixed and paraffin-embedded (FFPE) primary ccRCC tumor samples (Table 1); COHORT 2, 47 ccRCC FFPE tumor samples diagnosed as metastases (lung, 8; bone, 18; viscera, 11, brain, 4, and others, 6; Supplementary Table 1); and COHORT 3, 108 primary ccRCC tumor samples independently collected as an external validation cohort (Supplementary Table 2). COHORT 3 differed from COHORTS 1–2 in that an alcohol-based PAXgene (Qiagen) was used for fixation prior to paraffin embedding. The UICC TNM system was used for tumor staging, and nuclear grading was performed according to the WHO/International Society of Urological Pathology grading system. No statistical methods were used to predetermine the sample size. Tissue microarrays were created by a well-experienced board-certified pathologist (S.M.) who specializes in genitourinary malignancies and evaluated the suitability of tissue sections for tissue microarray construction. Tumor cores were punched from the central area of tumors and processed for further experiments. All samples were deciphered with numbers to avoid investigator bias during tissue preparation and data analyses. All procedures were performed in compliance with the 1964 Helsinki Declaration

Table 1 Characteristics of 105 patients with clear cell renal cell carcinoma (COHORT 1)

Characteristics	All ($n=105$)		Low risk ($n=21$, 20%)		Intermediate risk ($n=63$, 60%)		High risk ($n=21$, 20%)		p value
Age (median, IQR)	61 (53–71)		58 (52–73)		58 (53–70)		68 (55–76)		0.334
Gender (n, %)									0.909
Male	76	72.4%	16	76.2%	45	71.4%	15	71.4%	
Female	29	27.6%	5	23.8%	18	28.6%	6	28.6%	
Pathological T stage (n, %)									0.084
< pT3	64	61.0%	16	76.2%	39	61.9%	9	42.9%	
≥ pT3	41	39.0%	5	23.8%	24	38.1%	12	57.1%	
Tumor grade (n, %)									0.004
1/2	69	65.7%	18	85.7%	43	68.3%	8	38.1%	
3/4	36	34.3%	3	14.3%	20	31.7%	13	61.9%	
Venous invasion (n, %)									0.122
Yes	30	28.6%	3	14.3%	18	28.6%	9	42.9%	
No	75	71.4%	18	85.7%	45	71.4%	12	57.1%	

and present ethical standards, and informed consent for the experimental use of samples was obtained from patients according to the hospital's ethical guidelines.

Immunohistochemical staining and automated single-cell counting

Tissue microarray samples were cut into 5-µm-thick sections and placed onto silane-coated glass slides. After deparaffinization, sections were processed for antigen retrieval and blocking. Thereafter, all sections were incubated overnight with primary antibodies, followed by an incubation with secondary antibodies conjugated to a peroxidase-labeled dextran polymer. The primary antibodies used were as follows: anti-CD68 (#413,791, Nichirei, Tokyo, Japan), anti-CD163 (#ab182422, Abcam), anti-calreticulin (#ab92516, Abcam), anti-CD47 (#ab175388, Abcam), and anti-SIRPα (#ab53721, Abcam). Color development for immunohistochemistry was achieved using 3,3'-diaminobenzidine in 50 mM Tris–HCl (pH 5.5) containing 0.005% hydrogen peroxidase. Sections treated with 3,3'-diaminobenzidine were counterstained with hematoxylin. All stained sections were scanned using a high-resolution digital slide scanner (NanoZoomer-XR C12000; Hamamatsu Photonics, Hamamatsu, Shizuoka, Japan). Immunohistochemical signals and nuclei in tumor cores were separately segmented with a computerized image analysis system (StrataQuest software, Tissuegnostics, Vienna, Austria). Cells with overlapping segmented immune signals and nuclei were then automatically counted. A positive cell density indicates the mean number of positive cells in the defined tumor areas.

DNA extraction and sequencing

Genomic DNA was extracted from matched freshly frozen tissue samples for tissue microarrays with a DNeasy Blood & Tissue Kit (Qiagen) according to the manufacturer's protocol. The DNA integrity number was 4.0, which was calculated using the Agilent 2000 TapeStation (Agilent Technologies, Waldbronn, Germany). A genomic DNA library was constructed using GeneRead DNAseq Targeted Panel V2 (Human Comprehensive Cancer Panel), which covers more than 95% of the total exon region in 160 cancer-related genes [20–22]. We then used the GeneRead DNA I Amp Kit (Qiagen) and MiSeq (Illumina) for amplification and sequencing. FastQ files were analyzed using an original bioinformatics pipeline called GenomeJack (Mitsubishi Space Software, Tokyo, Japan), as previously described [23].

Statistical analysis

Continuous variables are presented as means with standard errors or as medians with interquartile ranges, and categorical variables are shown as frequencies with percentages. Variables between groups were compared using the Chi-squared test and Kruskal–Wallis H test, as appropriate. Spearman's coefficients were used to identify and evaluate the strength of relationships between the two sets of data. Uni- and multivariate Cox regression models with stepwise selection were used to evaluate variables associated with disease recurrence and overall mortality following surgery or disease progression and overall mortality following antiangiogenic tyrosine kinase inhibitors. Survival curves were estimated using the Kaplan–Meier method and compared with the Log-rank test. The significance of differences was accepted at $p < 0.05$. The c-index was calculated with Lifelines (version 0.27.4), a survival analysis package in Python (version 3.9.7). All analyses were performed using SPSS version 25.0 (IBM-SPSS Inc., Tokyo, Japan) and Python version 3.9.7 (Python Software Foundation, Wilmington, USA).

Results

Cell-by-cell innate immune signature analysis and outcomes

A quantitative immunohistological analysis enables the objective judgment of clinical data. We herein applied an automated single-cell count of immunolabeled tumor sections from 105 primary ccRCC in COHORT 1 (Table 1) via a virtual scanner. In this analysis, cells positive for CD68, CD163, the "eat me" signal calreticulin, the "don't eat me" signal CD47, and SIRPα were automatically distinguished and counted (Fig. 1a). Mean positive cell numbers in 105 ccRCC tumor samples were $866 \pm 674/mm^2$ for CD68, $541 \pm 609/mm^2$ for CD163, $219 \pm 487/mm^2$ for calreticulin, $1261 \pm 978/mm^2$ for CD47, and $113 \pm 200/mm^2$ for SIRPα. Positive correlations were observed between CD68 and CD163 only (Fig. 1b). Therefore, the varying expression patterns of the innate immune signatures indicated phenotypic differences in the innate immune state in patients with ccRCC.

We then investigated the effects of innate immune signatures on ccRCC patient survival following surgery. Among the five markers of innate immunity, a Kaplan–Meier analysis revealed a marked difference in overall mortality

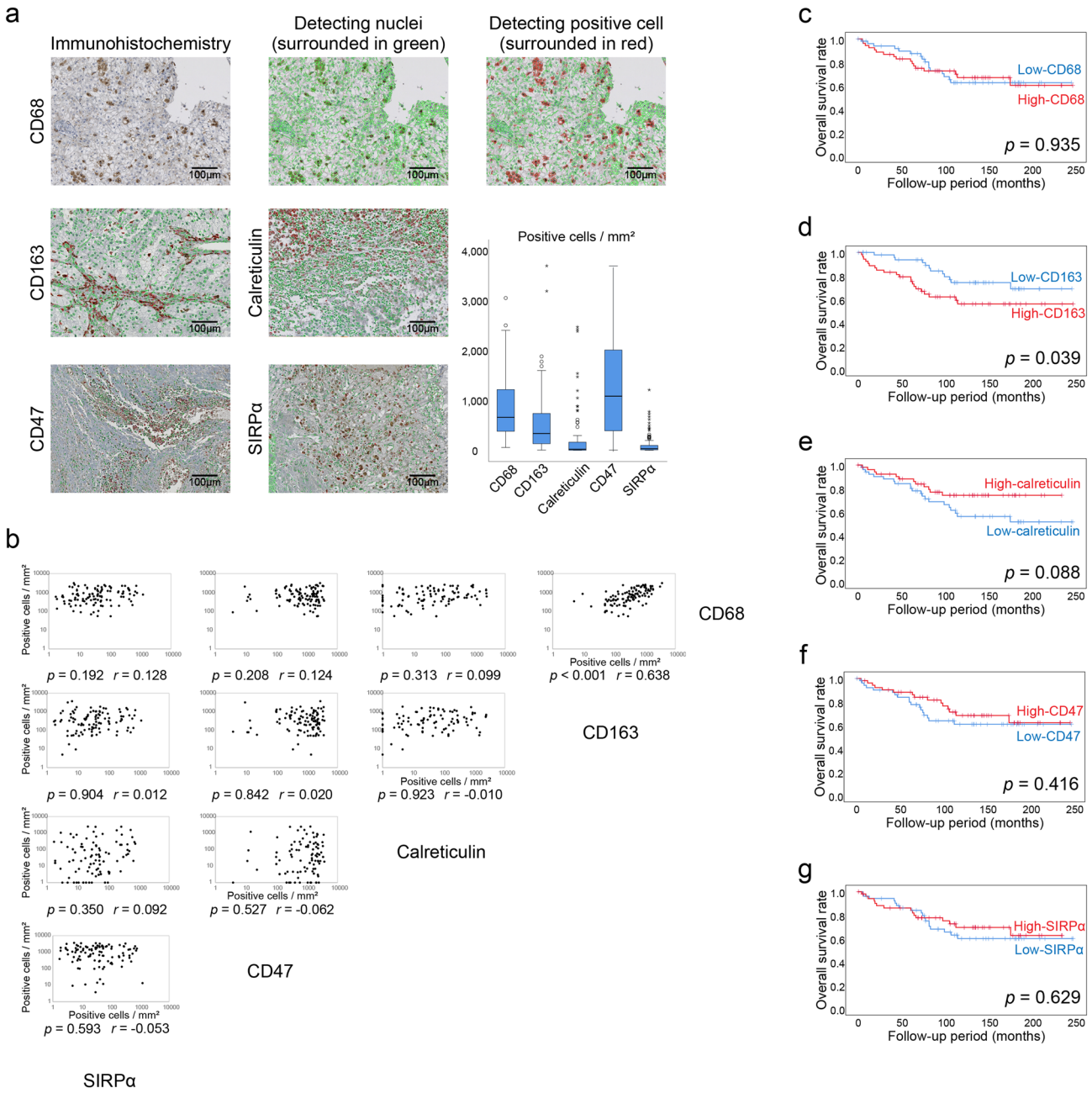

Fig. 1 Quantitative immunohistological evaluation and outcomes of ccRCC by automated single-cell counting. **a** Representative image of ccRCC displaying innate immune signatures for CD68, CD163, calreticulin, CD47, and SIRPα. Scale bar, 100 μm. **b** Summary of correlation coefficients in positive cell density between five innate immune signatures in 105 ccRCC patients (COHORT 1). **c–g** Kaplan–Meier curves for overall survival in 105 patients in COHORT 1 following surgery according to the indicated innate immune signatures: CD68 (**c**), CD163 (**d**), calreticulin (**e**), CD47 (**f**), and SIRPα (**g**). The *p* value was obtained from the Log-rank test

that correlated with CD163 expression and was associated with calreticulin expression (Fig. 1c–g). No significant differences were noted in overall mortality between CD68/CD47/SIRPα levels in surgically treated ccRCC.

Development of a new risk classification with prognostic innate immune signatures

Risk model optimization improves the accuracy of predictions on patient outcomes. Therefore, we assessed a new risk model based on the abovementioned innate immune signature information, i.e., CD163/calreticulin

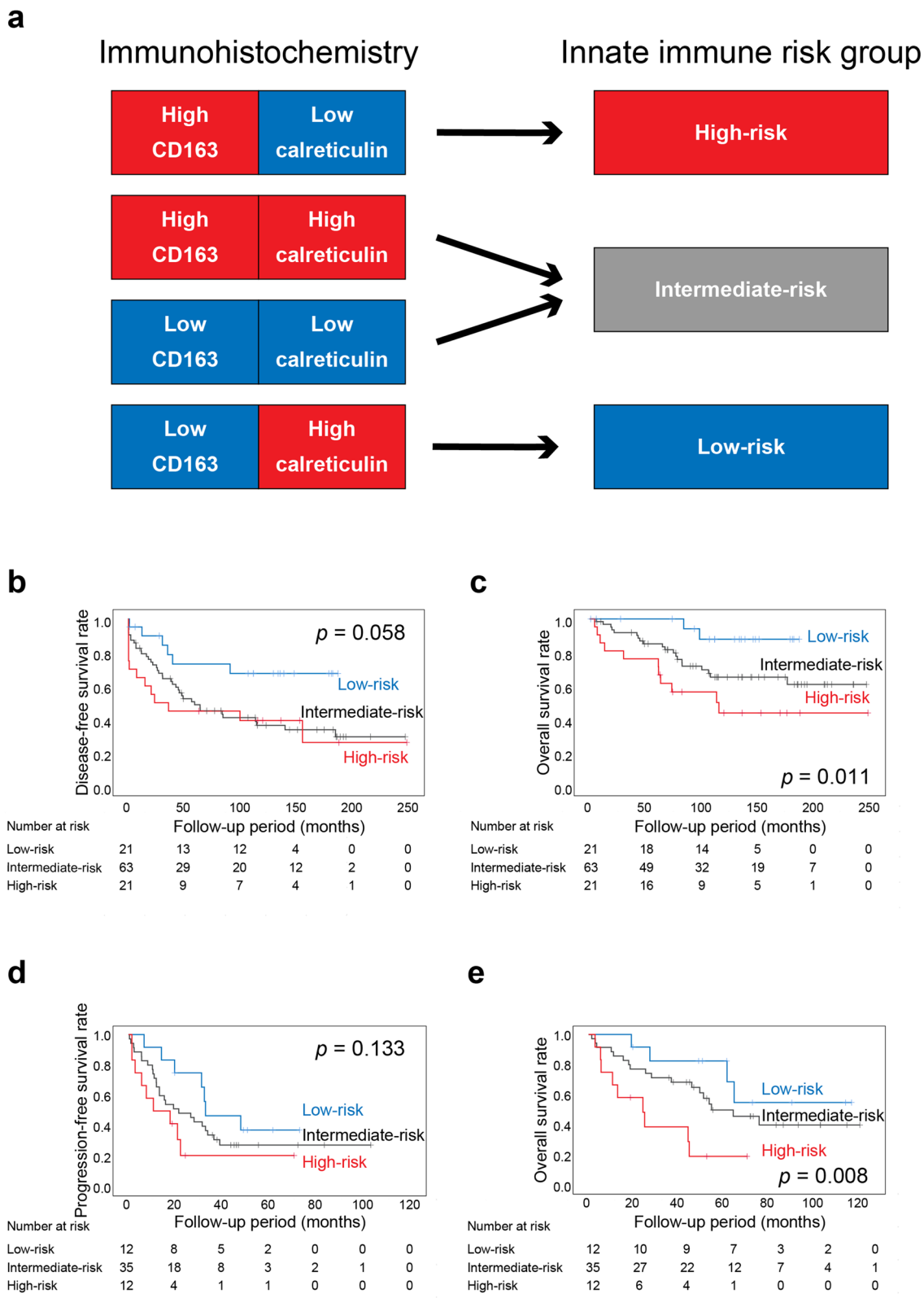

Fig. 2 Outcomes of patients with clear cell renal cell carcinoma according to three risk groups stratified by CD163/calreticulin levels. **a** Definition of the innate immune risk classification used. **b–c** Kaplan–Meier curves for disease-free survival (**b**) and overall survival (**c**) in 105 patients in COHORT 1 following surgery according to the indicated risk groups. **d–e** Kaplan–Meier curves for progression-free survival (**d**) and overall survival (**e**) in 59 recurrent patients in COHORT 1 following tyrosine kinase inhibitor treatments according to the indicated risk groups. The *p* value was obtained from the Log-rank test

levels, as summarized in Fig. 2a. In this risk stratification of COHORT 1, 21 patients (20%) were classified as low risk, 63 (60%) as intermediate risk, and 21 (20%) as high risk. Kaplan–Meier analyses based on the new risk group by CD163/calreticulin levels enabled the sequential stratification of patient prognosis, revealing that the innate immune risk group correlated with overall mortality ($p = 0.011$), but not disease recurrence following surgery ($p = 0.058$) (Fig. 2b–c). An examination of pathological features showed that the innate immune risk group, i.e., high CD163 and low calreticulin levels, correlated with a higher tumor grade ($p = 0.004$, Table 1). However, the multivariate analysis did not reveal any relationships between the innate immune risk group and patient prognosis following surgery independent of the pathological T stage and tumor grade for disease recurrence or patient age and tumor grade for overall mortality (Table 2).

Among 105 ccRCC patients, 59 (56%) received antiangiogenic tyrosine kinase inhibitors, including sorafenib and sunitinib, following disease relapse. Therefore, we investigated the relationship between sensitivity to tyrosine kinase inhibitor treatments and the current risk groups newly stratified by CD163/calreticulin levels. Kaplan–Meier analyses revealed that the innate immune risk group correlated with overall mortality ($p = 0.008$), but not disease progression following tyrosine kinase inhibitor treatments ($p = 0.133$) (Fig. 2d–e). Although the univariate analysis of disease progression following tyrosine kinase inhibitor treatments identified female sex as the only indicator in our population, in the multivariate analysis, the innate immune risk group (hazard ratio 4.871, $p = 0.006$, high vs. low; hazard ratio 2.828, $p = 0.029$, intermediate vs. low) also predicted disease progression following tyrosine kinase inhibitor treatments independent of the abovementioned factor, i.e., female sex

Table 2 Uni- and multivariate Cox regression analyses of 105 patients in COHORT 1 with clear cell renal cell carcinoma following surgery

Characteristic	Disease recurrence		*p* value	Overall mortality		*p* value
	Univariate *p* value	Multivariate HR (95% CI)		Univariate *p* value	Multivariate HR (95% CI)	
Age (≥ 60 vs. < 60 years)	0.196	1.362 (0.779–2.381)	0.279	0.017	2.358 (1.139–4.883)	0.021
Gender (female vs. male)	0.562	0.962 (0.532–1.741)	0.899	0.162	1.139 (0.522–2.485)	0.745
Pathological T stage (≥ pT3 vs. < pT3)	< 0.001	2.318 (1.298–4.138)	0.004	< 0.001	1.902 (0.861–4.203)	0.112
Tumor grade (3/4 vs. 1/2)	< 0.001	2.953 (1.677–5.199)	< 0.001	< 0.001	4.686 (2.296–9.563)	< 0.001
Venous invasion (yes vs. no)	0.102	0.762 (0.389–1.493)	0.428	0.083	0.830 (0.353–1.953)	0.669
Innate immune risk group	0.058		0.288	0.011		0.196
Low risk		Reference			Reference	
Intermediate risk	0.028	1.963 (0.818–4.712)	0.131	0.054	2.927 (0.676–12.663)	0.151
High risk	0.022	1.548 (0.563–4.253)	0.397	0.004	4.062 (0.876–18.838)	0.073

HR Hazard ratio; *CI* Confidence interval

Table 3 Uni- and multivariate Cox regression analyses of 59 patients in COHORT 1 with renal cell carcinoma following tyrosine kinase inhibitor treatments

Characteristic	Disease progression		*p* value	Overall mortality		*p* value
	Univariate *p* value	Multivariate HR (95% CI)		Univariate *p* value	Multivariate HR (95% CI)	
Age (≥ 60 vs. < 60 years)	0.530	1.528 (0.698–3.346)	0.289	0.788	1.026 (0.419–2.513)	0.955
Gender (female vs. male)	0.012	3.313 (1.560–7.036)	0.002	0.041	2.779 (1.277–6.048)	0.010
Pathological T stage (≥ pT3 vs. < pT3)	0.805	0.714 (0.316–1.616)	0.419	0.054	1.302 (0.506–3.349)	0.584
Tumor grade (3/4 vs. 1/2)	0.160	1.993 (0.983–4.043)	0.056	0.014	2.066 (0.712–5.994)	0.182
Venous invasion (yes vs. no)	0.778	0.492 (0.226–1.070)	0.073	0.421	0.610 (0.252–1.478)	0.274
Innate immune risk group	0.133		0.013	0.008		0.006
Low risk		Reference			Reference	
Intermediate risk	0.233	2.828 (1.112–7.188)	0.029	0.264	2.101 (0.705–6.260)	0.182
High risk	0.038	4.871 (1.587–14.950)	0.006	0.006	6.782 (1.950–23.589)	0.003

HR Hazard ratio; *CI* Confidence interval

(Table 3). Furthermore, uni- and multivariate analyses of overall mortality following tyrosine kinase inhibitor treatments showed similar results, indicating that the innate immune risk group predicted overall mortality (hazard ratio 6.782, $p=0.003$, high vs. low; hazard ratio 2.101, $p=0.182$, intermediate vs. low) independent of female sex (Table 3). Calculating the concordance index (c-index) of the innate immune risk model yielded 0.74 for overall mortality, which revealed the best performance compared to models with clinicopathological parameters plus CD163 value (c-index 0.72) or calreticulin value (c-index 0.71).

Collectively, these results demonstrate that the current risk groups stratified by CD163/calreticulin levels predict the outcomes of ccRCC patients, particularly those receiving tyrosine kinase inhibitor treatments, suggesting that patients with high CD163 and low calreticulin levels are resistant to antiangiogenic therapy.

Prognostic innate immune signatures in metastases

We investigated current innate immune signatures, i.e., CD163 and calreticulin, in the metastatic ccRCC tumor space to clarify site-specific differences in the tumor immune microenvironment. Using metastatic ccRCC specimens consisting of 47 samples (COHORT 2; Supplementary Table 1), we initially assessed the automated single-cell count of CD163 and calreticulin expression (Fig. 3a). No correlations were observed between CD163 and calreticulin expression levels in ccRCC metastasis, which was consistent with the findings obtained for primary kidney tumors. In our risk stratification of COHORT 2, 4 patients (9%) were classified as low risk, 25 (53%) as intermediate risk, and 18 (38%) as high risk. Tumor metastases had a higher innate immune risk in ccRCC than primary lesion ($p=0.032$) (Fig. 3b). Varying patterns of CD163/calreticulin risk groups were revealed for each site, with 50% of ccRCC lung metastases being classified into the high-risk group.

Validation of effects of CD163 and calreticulin on ccRCC prognosis

To confirm the effects of CD163 and calreticulin expression levels in ccRCC, we attempted to validate our hypothesis using an external validation dataset containing in-house primary ccRCC samples, namely, COHORT 3 ($n=108$; Supplementary Table 2). In our risk stratification of COHORT 3, 36 patients (33%) were classified as low risk, 57 (53%) as intermediate risk, and 15 (14%) as high risk. A prognostic analysis of validated COHORT 3 showed similar results, revealing that the innate immune risk group correlated with overall mortality ($p=0.040$), but not disease recurrence following surgery ($p=0.113$) (Fig. 4b–c). Although tumor characteristics in COHORT 3 differed from those in

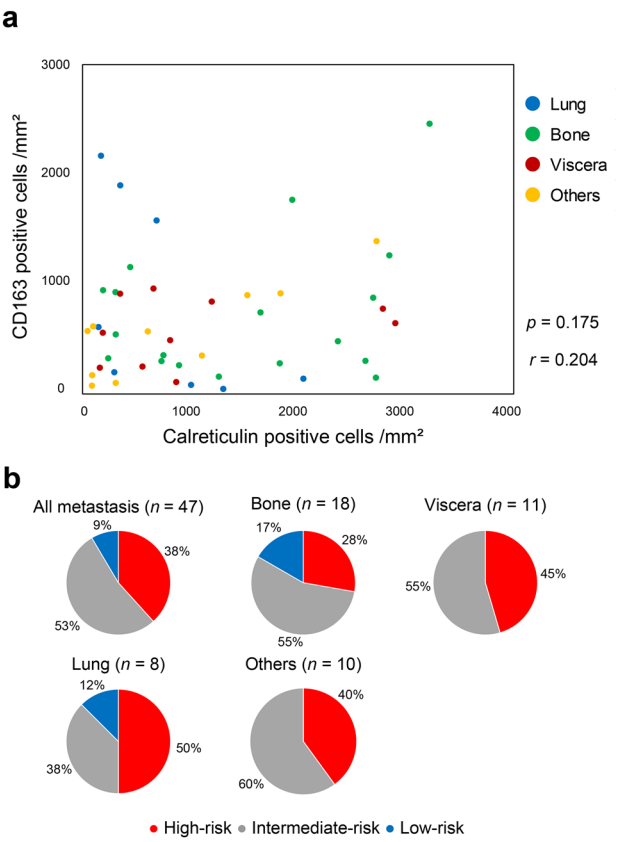

Fig. 3 Site-specific differences in the expression of innate immune signatures CD163 and calreticulin in ccRCC metastases. **a** Scatter plots show the density of $CD163^+$ and $calreticulin^+$ cells ($/mm^2$) in 47 metastatic ccRCC samples (COHORT 2). **b** Inferred risk group distributions obtained in (**a**) by metastatic regions

COHORT 1 (Supplementary Table 2), we achieved similarly good discrimination in screening patients with a poor prognosis using our innate immune risk group.

Genomic landscapes related to innate immune signatures

An analysis of the genomic alterations responsible for current high-risk tumors revealed the prominent features of ccRCC tumors that may serve as potential biomarkers for the targeting of innate immunity. We examined 55 ccRCC samples from two cohorts, COHORTS 1 and 3, for alterations in 160 cancer-associated genes, depending on our innate immunity risk stratification (Fig. 5a). The most frequently altered genes in our ccRCC tumor samples were VHL, PBRM1, SETD2, ATM, and MTOR. When we examined typical cancer-related pathways, we found that alterations in the TP53/cell cycle pathway were highly prevalent in the high-risk tumor group (Fig. 5b), occurring in 38% of patients compared with 11% in patients at low and intermediate risk. However, no significant differences were noted in

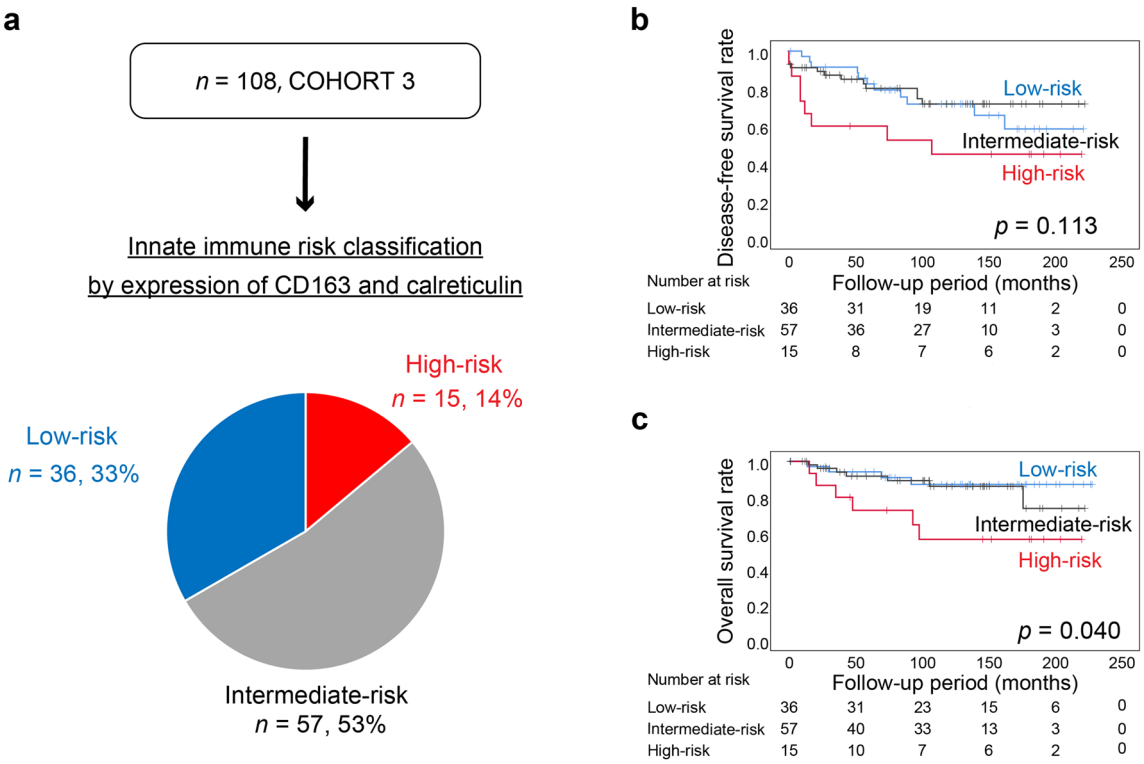

Fig. 4 Validation of effects of innate immune signatures on the prognosis of ccRCC. **a** Immunohistochemical study and risk stratification for the expression of innate immune signatures CD163 and calreticulin in the validated COHORT 3 dataset. **b-c** Kaplan–Meier curves for disease-free survival (**b**) and overall survival (**c**) in 108 patients in COHORT 3 following surgery according to the indicated risk groups. The *p* value was obtained from the Log-rank test

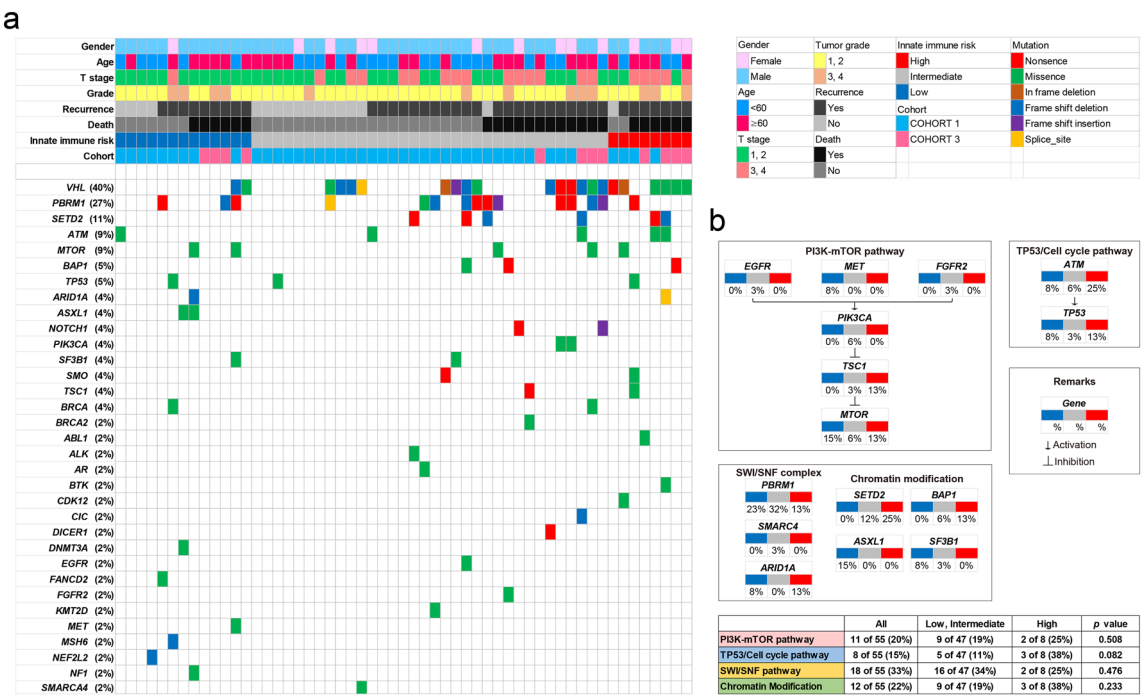

	All	Low, Intermediate	High	*p* value
PI3K-mTOR pathway	11 of 55 (20%)	9 of 47 (19%)	2 of 8 (25%)	0.508
TP53/Cell cycle pathway	8 of 55 (15%)	5 of 47 (11%)	3 of 8 (38%)	0.082
SWI/SNF pathway	18 of 55 (33%)	16 of 47 (34%)	2 of 8 (25%)	0.476
Chromatin Modification	12 of 55 (22%)	9 of 47 (19%)	3 of 8 (38%)	0.233

Fig. 5 Relationship between the innate immune risk group and genetic alterations in ccRCC patients. **a** Genomic alterations in tumorigenic signaling pathways related to the development of ccRCC in the innate immune risk groups. **b** Percentage of samples with alterations in each of the selected signaling pathways

the subsets of PI3K-mTOR pathway genes, SWI/SNF complex genes, or chromatin-modifying genes between the two groups (Fig. 5b).

Discussion

After successful clinical trials on the immune checkpoint inhibitors PD-1/PD-L1/CTLA-4, immunotherapy targeting innate immunity has attracted attention. Since combination therapy with the immune checkpoint inhibitor 5F9, which blocks CD47, and rituximab achieved a complete response rate of 36% in non-Hodgkin's lymphoma patients, various trials targeting the innate immunity axis are now being conducted on many cancers, from hematological malignancies to solid tumors [14–16]. In the present study, we evaluated five representative markers of innate immunity and demonstrated that CD163 and the "eat me" signal calreticulin were valuable for predicting the outcomes of ccRCC patients. Our new risk classification based on CD163 and calreticulin levels may be used to predict oncological outcomes in ccRCC patients who underwent surgery and received tyrosine kinase inhibitor treatments. Furthermore, we reported genomic alteration profiles based on the CD163 and calreticulin states, revealing marked differences in TP53/Cell cycle pathway alterations, implying genetic interactions between these molecules and tumor innate immunity within ccRCC tumors.

Chevrier et al. clarified the immune profile of ccRCC using mass cytometry with extensive antibody panels and for the first time revealed the distinct characteristics of TAMs [24]. Seventeen major phenotypes of TAMs were identified, and a subset of the cluster had a strong relationship with exhausted T cells, indicating poor survival. Regarding the relationship between innate immunity and the prognosis of RCC, Komohara et al. demonstrated that high expression levels of CD163, a specific marker for TAMs, were associated with poor overall survival in 66 cohorts of ccRCC patients [25]. Additionally, Ma et al. showed that high CD163 expression levels in tumor beds were associated with an advanced tumor stage, disease recurrence, and overall mortality in surgically resected ccRCC patients [26]. Furthermore, Hua et al. proposed a unique risk classification based on immune-related genes to predict the overall survival of ccRCC patients, showing that CD47 positively correlated with an increased risk of mortality [27]. In a preclinical study, Yanagita et al. showed that SIRPα was highly expressed in human ccRCC and that an antibody against SIRPα attenuated the growth of SIRPα-expressing RCC tumors in a syngenetic mouse model [28]. In summary, further studies are needed to elucidate the innate immunity of RCC in more detail.

We herein discuss three major results that may be translated into future clinical practice. The anti-PD-1/PD-L1/CTLA-4 antibody strongly impacted ccRCC treatment; however, the response rate was not sufficiently high [9, 10]. Therefore, it is important to search for the next targets following existing immune-oncology drugs. The present results suggest that CD163 and calreticulin, markers of tumor innate immunity, have potential as new therapeutic targets of ccRCC because high CD163 and low calreticulin expression levels correlated with a higher tumor grade. Furthermore, we derived a new risk classification based on the levels of the innate immune signatures CD163/calreticulin in ccRCC. This so-called innate immune risk group correlated with overall mortality following surgery, and this risk classification may be used to stratify possible candidates for adjuvant therapy or to create an appropriate follow-up plan. Notably, since the innate immune risk group was associated with the prognosis of ccRCC patients receiving antiangiogenic tyrosine kinase inhibitors, our risk classification may be helpful for the selection of ccRCC patients as candidates for future tyrosine kinase inhibitors or other alternative therapies, including immune-oncology therapy. Moreover, although some organ-specific differences were observed, metastases appeared to have a higher innate immune risk. In the lungs, i.e., the most common site of metastasis in ccRCC, 50% of patients were classified into the high-risk group according to our risk score. This information may allow for more precise medical care when considering novel therapies based on innate immunity.

In summary, we evaluated five representative innate immune markers, CD68, CD163, calreticulin, CD47, and SIRPα, by automated single-cell pathology and demonstrated that the combination of CD163 and calreticulin levels showed the best performance to predict ccRCC outcomes. Furthermore, tumors with high CD163 and low calreticulin expression levels correlated with a higher tumor grade in ccRCC. We revealed a relationship between CD163/calreticulin levels in tumor beds and sensitivity to antiangiogenic therapy in ccRCC patients receiving tyrosine kinase inhibitors. After the advent of immune-oncology treatment, immunity has become the hottest area in cancer treatment. The present results provide novel insights into the immunobiology of ccRCC tumors and will contribute to the development of future therapy that focuses on innate immunity in solid cancers. However, some limitations need to be addressed. This study was a retrospective analysis that included a small number of patients. Furthermore, there was the lack of involvement of multiple pathologists in tissue microarray creation. In addition, few data are available to biologically support the cancerous effects of innate immunity CD163 and calreticulin expression on patient outcomes in ccRCC. Therefore, further studies, including prospective studies and/

or validations of large datasets, are needed to provide robust evidence related the innate immune system in ccRCC.

Supplementary Information The online version contains supplementary material available at https://doi.org/10.1007/s00262-023-03369-8.

Acknowledgements The present study was supported by Grants-in-Aid for Scientific Research (KAKENHI 21K09411 to T.A.; 19H03792, 21K19414, and 22H03217 to N.T), the Takeda Science Foundation (N.T.), the Kobayashi Foundation for Cancer Research (N.T.), the SGH Foundation for Cancer Research (to N.T.), the Princess Takamatsu Cancer Research Fund (to N.T.), and the Keio Gijuku Academic Development Funds (to N.T.).

Author contributions T.A. and N.T. designed the study. T.A., K.T., K.H., R.K., Y.B., and S.M. performed the experiments. T.T., K.M., S.M., T.K., and R.M. provided conceptual advice. H.N. performed genetic experiments. T.A. and N.T. wrote the manuscript with inputs from M.O.

Declarations

Competing interests The authors declare no competing interests.

Conflict of interest The authors declare no competing interests.

References

1. Choueiri TK, Motzer RJ (2017) Systemic therapy for metastatic renal-cell carcinoma. N Engl J Med 376:354–366
2. Medical Research Council Renal Cancer Collaborators (1999) Interferon-alpha and survival in metastatic renal carcinoma: early results of a randomised controlled trial. Medical Research Council Renal Cancer Collaborators. Lancet 353:14–17
3. Klapper JA, Downey SG, Smith FO et al (2008) High-dose interleukin-2 for the treatment of metastatic renal cell carcinoma : a retrospective analysis of response and survival in patients treated in the surgery branch at the National Cancer Institute between 1986 and 2006. Cancer 113:293–301
4. Motzer RJ, Hutson TE, Tomczak P et al (2007) Sunitinib versus interferon alfa in metastatic renal-cell carcinoma. N Engl J Med 356:115–124
5. Escudier B, Eisen T, Stadler WM et al (2007) Sorafenib in advanced clear-cell renal-cell carcinoma. N Engl J Med 356:125–134
6. Hudes G, Carducci M, Tomczak P et al (2007) Temsirolimus, interferon alfa, or both for advanced renal-cell carcinoma. N Engl J Med 356:2271–2281
7. Motzer RJ, Escudier B, Oudard S et al (2008) efficacy of everolimus in advanced renal cell carcinoma: a double-blind, randomised, placebo-controlled phase iii trial. Lancet 372:449–456
8. Motzer RJ, Hutson TE, Cella D et al (2013) Pazopanib versus sunitinib in metastatic renal-cell carcinoma. N Engl J Med 369:722–731
9. Motzer RJ, Escudier B, McDermott DF et al (2015) Nivolumab versus everolimus in advanced renal-cell carcinoma. N Engl J Med 373:1803–1813
10. Motzer RJ, Tannir NM, McDermott DF et al (2018) Nivolumab plus ipilimumab versus sunitinib in advanced renal-cell carcinoma. N Engl J Med 378:1277–1290
11. Chen DS, Mellman I (2013) Oncology meets immunology: the cancer-immunity cycle. Immunity 39:1–10
12. Kim JM, Chen DS (2016) Immune escape to PD-L1/PD-1 blockade: seven steps to success (or failure). Ann Oncol 27:1492–1504
13. Feng M, Jiang W, Kim BYS et al (2019) Phagocytosis checkpoints as new targets for cancer immunotherapy. Nat Rev Cancer 19:568–586
14. Advani R, Flinn I, Popplewell L et al (2018) CD47 blockade by Hu5F9-G4 and rituximab in non-Hodgkin's lymphoma. N Engl J Med 379:1711–1721
15. Weiskopf K (2017) Cancer immunotherapy targeting the CD47/SIRPalpha axis. Eur J Cancer 76:100–109
16. Chao MP, Takimoto CH, Feng DD et al (2019) Therapeutic targeting of the macrophage immune checkpoint CD47 in myeloid malignancies. Front Oncol 9:1380
17. Mantovani A, Longo DL (2018) Macrophage checkpoint blockade in cancer—back to the future. N Engl J Med 379:1777–1779
18. Mantovani A, Marchesi F, Malesci A et al (2017) Tumour-associated macrophages as treatment targets in oncology. Nat Rev Clin Oncol 14:399–416
19. Schcolnik-Cabrera A, Oldak B, Juarez M et al (2019) Calreticulin in phagocytosis and cancer: opposite roles in immune response outcomes. Apoptosis 24:245–255
20. Takamatsu K, Tanaka N, Hakozaki K et al (2021) Profiling the inhibitory receptors LAG-3, TIM-3, and TIGIT in renal cell carcinoma reveals malignancy. Nat Commun 12:5547
21. Masuda T, Tanaka N, Takamatsu K et al (2022) Unique characteristics of tertiary lymphoid structures in kidney clear cell carcinoma: prognostic outcome and comparison with bladder cancer. J Immunother Cancer 10:e003883
22. Kufukihara R, Tanaka N, Takamatsu K et al (2022) Hybridisation chain reaction-based visualisation and screening for lncRNA profiles in clear-cell renal-cell carcinoma. Br J Cancer 127:1133–1141
23. Hakozaki K, Tanaka N, Takamatsu K et al (2021) Landscape of prognostic signatures and immunogenomics of the AXL/GAS6 axis in renal cell carcinoma. Br J Cancer 125:1533–1543
24. Chevrier S, Levine JH, Zanotelli VRT et al (2017) An immune atlas of clear cell renal cell carcinoma. Cell 169(736–749):e718
25. Komohara Y, Hasita H, Ohnishi K et al (2011) Macrophage infiltration and its prognostic relevance in clear cell renal cell carcinoma. Cancer Sci 102:1424–1431
26. Ma C, Horlad H, Ohnishi K et al (2018) CD163-positive cancer cells are potentially associated with high malignant potential in clear cell renal cell carcinoma. Med Mol Morphol 51:13–20
27. Hua X, Chen J, Su Y, Liang C (2020) Identification of an immune-related risk signature for predicting prognosis in clear cell renal cell carcinoma. Aging (Albany NY) 12:2302–2332
28. Yanagita T, Murata Y, Tanaka D et al (2017) Anti-SIRPalpha antibodies as a potential new tool for cancer immunotherapy. JCI Insight 2:e89140